Editors' Suggestion

Probing laser-induced spin-current generation in synthetic ferrimagnets using spin waves

Tom Lichtenberg,[1,*] Youri L. W. van Hees,[1,*] Maarten Beens,[1] Caspar J. Levels,[1] Reinoud Lavrijsen,[1] Rembert A. Duine,[1,2] and Bert Koopmans[1]

[1]*Department of Applied Physics, Eindhoven University of Technology, P.O. Box 513, 5600 MB Eindhoven, The Netherlands*

[2]*Institute for Theoretical Physics, Utrecht University, Leuvenlaan 4, 3584 CE Utrecht, The Netherlands*

(Received 22 June 2022; accepted 14 September 2022; published 30 September 2022)

Several rare-earth transition-metal ferrimagnetic systems exhibit all-optical magnetization switching upon excitation with a femtosecond laser pulse. Although this phenomenon is very promising for future optomagnetic data storage applications, the role of nonlocal spin transport in these systems is scarcely understood. Using Co/Gd and Co/Tb bilayers, we isolate the contribution of the rare-earth materials to the generated spin currents by using the precessional dynamics they excite in an adjacent ferromagnetic layer as a probe. By measuring terahertz (THz) standing spin-waves as well as GHz homogeneous precessional modes, we probe both the high- and low-frequency components of these spin currents. The low-frequency homogeneous mode indicates a significant contribution of Gd to the spin current but not from Tb, consistent with the difficulty in achieving all-optical switching in Tb-containing systems. Measurements on the THz frequency spin waves reveal the inability of the rare-earth generated spin currents to excite dynamics at the subpicosecond timescale. We present modeling efforts using the $s-d$ model, which effectively reproduces our results and allows us to explain the behavior in terms of the temporal profile of the spin current.

DOI: 10.1103/PhysRevB.106.094436

I. INTRODUCTION

Over the past few decades, femtosecond (fs) laser excitation of magnetic materials has led to the discovery of a rich collection of physical phenomena. Among these, single fs laser pulse all-optical switching (AOS) of the magnetization in rare-earth transition-metal ferrimagnetic alloys [1,2] and multilayers [3,4] appears to be especially promising for future memory applications [5]. This phenomenon was shown to arise from the transfer of angular momentum between two magnetic sublattices [6]. In the same period the fs laser excitation of spin currents, mobile electrons carrying spin angular momentum, has been gaining significant interest from a fundamental perspective [7,8].

A particularly relevant use for these optically excited spin currents exploits their ability to transfer angular momentum between two ferromagnetic layers. This was first demonstrated in an experiment investigating the ultrafast laser induced magnetization dynamics of two ferromagnetic layers separated by a conductive spacer layer [9]. A diverse body of research into optically generated spin currents has since arisen [7,10–15]. In recent years, it has been shown that novel device functionality can be achieved at the intersection of AOS and optically excited spin currents. These works focus on systems where an all-optically switchable ferrimagnetic layer is separated by a spacer layer from a ferromagnetic layer. Depending on the precise composition of the layers, either the spin current coming from the ferromagnet can influence the AOS process [16] or the ferromagnet can be switched by the spin current coming from the switchable layer [17–19]. This last case demonstrates the strength of the spin current generated upon excitation of an all-optically switchable system and begs the question to what extent this spin current plays a role in the switching mechanism.

Although a great deal of AOS research has been performed on Gd(Fe)Co and Co/Gd systems, recent research indicates that Tb can be used as rare-earth (RE) component instead of Gd [4,20]. However, in these works, AOS has been found only for very specific layer thicknesses, a requirement which is not present in layered ferrimagnets containing Gd [21]. Work by Choi *et al.* has shown that spin currents generation in Tb is significantly weaker than in Gd [22], hinting at an explanation for the increased difficulty in attaining AOS. Here the accumulation of spins at the far end of a thick conductive spacer layer was measured, which can lead to a distorted spin current profile due to diffusive electron transport [8]. Moreover, the use of alloys makes it difficult to disentangle the spin current contributions originating from different elements.

In this work, we systematically study spin current generation in synthetic ferrimagnets using the collective spin precession they excite in a neighboring layer as a probe. The basic experimental concept and the noncollinear magnetic bilayers used in this work are sketched in Fig. 1(a). The generation layers are synthetic ferrimagnetic bilayers, consisting of Co which couples antiferromagnetically to either Gd or Tb. Although these latter materials are paramagnetic at room temperature in bulk, a ferromagnetic phase can be stabilized when interfaced with a ferromagnetic material [23], which decays exponentially away from the interface. Upon laser excitation of the out-of-plane magnetized generation layer, a spin current which is spin-polarized in the direction

[*]These authors contributed equally.

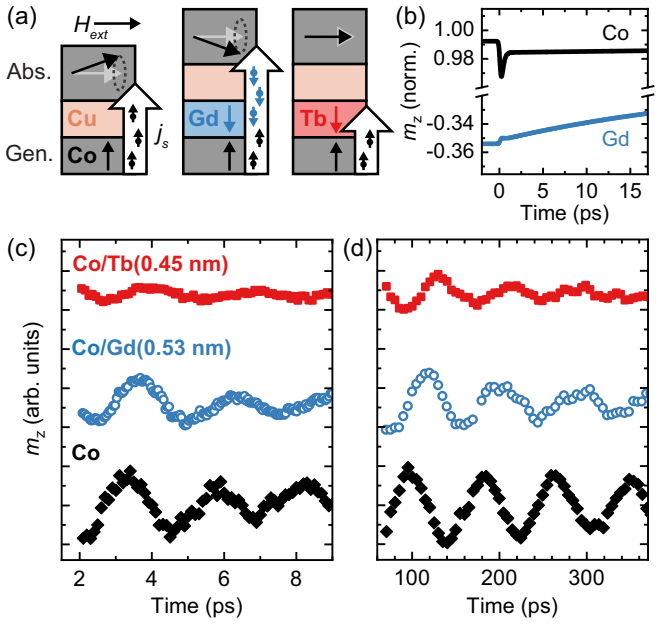

FIG. 1. (a) Schematic overview of the experiments, where the effect of the generation layer composition on the response of the absorption layer is sketched for each of the three studied configurations (Co, Co/Gd, and Co/Tb). (b) Example magnetization response calculated using the *s-d* model for Co and for Gd in a Co/Gd bilayer. [(c) and (d)] Response of the absorption layer for each studied configuration. Both (c) the homogeneous ($H_{\text{ext}} = 100$ mT) and (d) the first order inhomogeneous mode ($H_{\text{ext}} = 0$ mT) are plotted, where the latter is measured using *complex MOKE*.

of the local magnetization is excited and injected into a ferromagnetic absorption layer with in-plane magnetization. There the spins exert a torque on the local magnetic moments and excite both the homogeneous precessional mode [8,24] as well as higher-order inhomogeneous spin waves [25,26]. By extracting the phase, amplitude and frequency of the FMR mode and THz spin waves, we indirectly study the absorbed spin current [27], which is commonly expected to scale with the time derivative of the magnetization (dm/dt), fulfilling conservation of angular momentum [8,27]. In this framework, these spin-wave parameters are directly proportional to the corresponding parameters of the Fourier component of the spin-torque pulse at the spin-wave frequency. Specifically, we probe the phase of the precessional dynamics to investigate the temporal profile of the spin current, and the amplitude to study the spin-current strength and attenuation. Changing the thickness of the RE layer changes both spin-current properties, which leads to significant variations in the measured parameters of the precessions. By measuring both the homogeneous FMR mode (∼10 GHz) and the first-order inhomogeneous mode (∼0.5 THz), the spin current can be studied on two distinct timescales, giving access to both the fast as well as the slow components of the spin current separately. We corroborate our experiments with an $s-d$ model, which treats local and nonlocal spin dynamics in a joint description [28–31].

Our results on the FMR mode show a strong contribution to the excited spin current from Gd, which is in line with previous work [17,22] and confirmed by our modeling efforts. In contrast, the THz mode cannot be efficiently excited by Gd, hinting at the relatively slow nature of the spin current contribution from Gd. In the Co/Tb system, both the FMR and THz modes are found to vanish with only a slight addition of Tb, indicating weak spin current generation in Tb but strong spin absorption, consistent with the high spin-orbit coupling (SOC) in this material. These results shed new light on nonlocal spin dynamics in highly technologically relevant synthetic ferrimagnets, and help elucidate the role of these processes in all-optical magnetic data recording.

II. EXPERIMENTAL DETAILS

The noncollinear magnetic bilayer central to this work, as sketched in Fig. 1(a), consists of an out-of-plane magnetized Co/RE generation layer (where RE is either Gd or Tb) and an in-plane magnetized Co absorption layer. Spin transport between the two magnetic layers is facilitated by a thin Cu spacer layer, which also serves to magnetically decouple the layers. The samples are fabricated using DC magnetron sputtering, where we vary the RE layer thickness along the sample length to ensure consistency between measurements. The full sample stack is given by Si:B(substrate)/Ta(4)/Pt(4)/Co(1)/RE(X)/Cu(2.5)/Co(5)/Pt(2.5) (numbers in brackets indicate the thickness in nm, with X being the variable RE thickness).

We employ pump-probe spectroscopy to measure the magnetization dynamics upon laser-pulse excitation, using the magneto-optical Kerr effect (MOKE) in the polar configuration to probe the magnetization. The sample is placed in a magnetic field with a variable angle of up to 20° with the sample plane. A mode-locked Ti:Sapphire laser is used to generate pulses at a repetition rate of 80 MHz and with a wavelength of 780 nm. The pulse length at sample position is approximately 150 fs. Both pump and probe pulses are focused onto the sample with a spot size of approximately 16 and 8 μm^2, respectively, and the pump fluence is about 1 mJ/cm^2. We use *Complex MOKE* to separate the magnetic contrast of both magnetic layers [32]. To accurately determine the absolute spin-wave phase in our experiments, the so-called coherence peak is used, which arises at temporal and spatial pump-probe overlap due to interference effects [33]. For more details on the experimental setup, see Sec. I of Ref. [34].

III. EXPERIMENTAL RESULTS

As a first experiment, we investigate the general behavior of the precessional dynamics for the three different generation layer configurations [Fig. 1(a)]. In order to isolate the contribution of the RE layers, in which the magnetization decays exponentially away from the Co interface, their thicknesses need to be chosen carefully. Previous work gives a typical lengthscale of the magnetization decay in Gd of 0.45 nm [3], with a similar value to be expected for Tb. In Figs. 1(c) and 1(d), we present typical measurements of the THz spin-wave and FMR mode respectively for the three different generation layer configurations, namely Co(1), Co(1)/Gd(0.53), and Co(1)/Tb(0.45). Our results show that the composition of the generation layer significantly influences the spin-wave

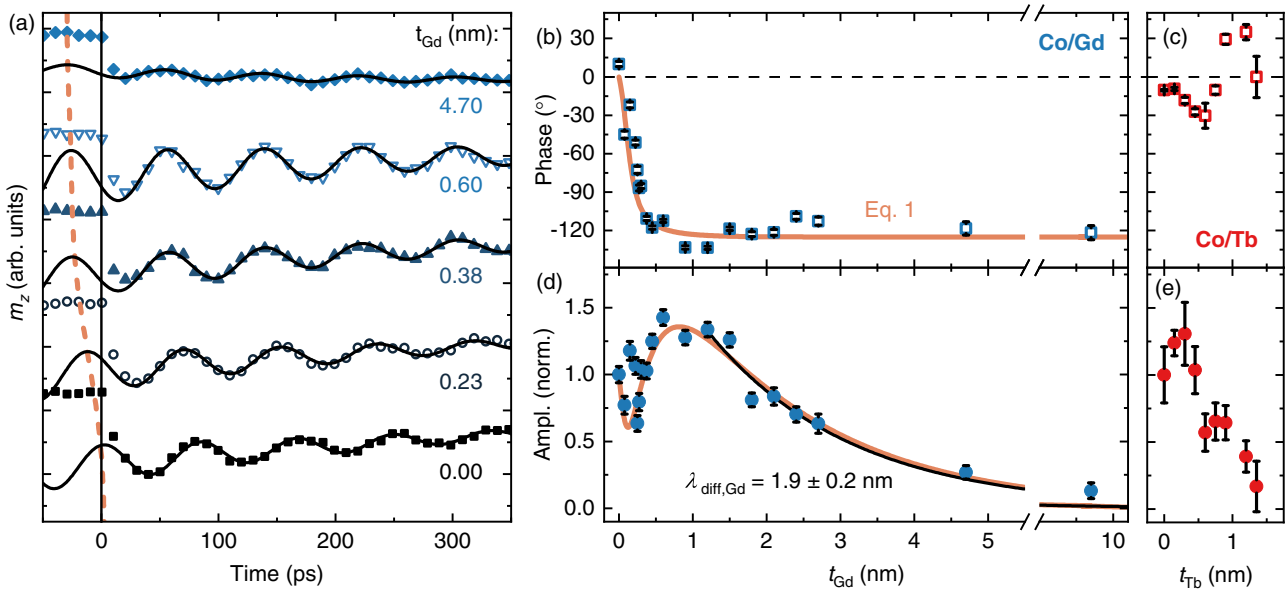

FIG. 2. (a) Measured FMR mode (H_{ext} = 100 mT) for several Gd thicknesses, fitted with a damped cosine function. The orange dashed line indicates the FMR phase shift and the thickness calibration is discussed in Sec. I of Ref. [34]. [(b) and (c)] FMR phase as a function of Gd (b) and Tb (c) thickness. [(d) and (e)] FMR amplitude as a function of Gd (d) and Tb (e) thickness, normalized to the amplitude without RE layer for both datasets. The orange solid line in (b) and (d) represents the modeled behavior using Eq. (1), and the black solid line in (d) is a fit with an exponential function.

behavior, specifically the amplitude and phase. To better understand this observation, we show representative modelled traces (see Sec V of Ref. [34]) of the magnetization response of Co and Gd upon fs laser excitation, in Fig. 1(b). The precessional behavior can then generally be understood with a simple picture where the generated spin current is assumed to be proportional to dm/dt [8,27]. Considering the antiferromagnetic coupling between Co and Gd (or Tb), the spin currents generated by the RE material and by Co should also have the opposite sign. Therefore we expect that the polarization of the total spin current changes sign (Fig. 1(a)) when the RE material becomes the dominant contributor, which could explain the experimental observation of the large phase shift of the FMR mode. However, no such sign change is observed in the THz measurements, hinting at a less significant contribution of the RE material to the subpicosecond spin current dynamics. This is consistent with the expected magnetization dynamics plotted in Fig. 1(b), which for Gd take place on the timescale of multiple ps, leading to a relatively slow spin current profile. Additionally, we find a strongly reduced amplitude for precession excited with a Co/Tb generation layer. This can be attributed to strong absorption of the spin current generated in Co, consistent with the large SOC in Tb [35,36], which has also been used to explain the relatively fast laser-induced dynamics of Tb, as well as weak spin current generation.

A. FMR mode

To get a better understanding of the observed behavior, we systematically measure both the FMR and THz mode as a function of the Gd and Tb thickness in the generation layer. First we discuss the results on the FMR mode, of which we show a selection of measurements for a Co(1)/Gd(X) generation layer in Fig. 2(a). To extract the phase and amplitude of the FMR mode, these measurements are fitted with a damped cosine function, indicated by the solid black lines, where the frequency is shared between all datasets.

We first discuss the FMR mode phase, of which we already observe a shift as a function of Gd thickness in Fig. 2(a), as indicated by the dotted orange line connecting the shifted maxima of the fits. The phase we extract from the fits is plotted in Figs. 2(b) and 2(c) for Co/Gd and Co/Tb respectively. With the addition of only 1 nm of Gd, a phase shift of more than 130° is observed, whereas no consistent phase shift is measured when adding Tb. This again indicates a strong contribution to the spin current from Gd, but a small to nonexistent contribution from Tb. For large thicknesses of Gd, the phase remains constant, which can be explained by the paramagnetic state further away from the Co/Gd interface.

Next, we focus on the amplitude of the FMR mode as a function of RE thickness, which is normalized to the amplitude for a pure Co generation layer and plotted in Figs. 2(d) and 2(e) for Co/Gd and Co/Tb, respectively. This amplitude has been corrected for changes in light absorption using transfer matrix calculations [37], as described in Sec. II of Ref. [34]. For Gd, an initial dip and successive rise of the amplitude are observed, followed by a gradual decrease. This behavior, in combination with the observed change of the FMR phase can be captured in a simple toy model where we assume the spin current contributions from Co and Gd excite two spin waves with different amplitudes and phases, but with the same frequency. As discussed previously, the Gd is magnetized due to exchange coupling with the Co, decaying at a characteristic length scale λ_{mag} which determines its contribution to the total spin current. Furthermore, the addition of Gd introduces a characteristic length scale λ_{diff} over which spin information is lost due to spin flip scattering events, known

as the spin diffusion length. For now we assume that spin diffusion is independent of the magnetic state of Gd. Writing the phase difference δ between the two excited precessions using Euler's formula, the FMR mode can then be described as

$$A_{\mathrm{FMR}}\, e^{i\phi} = \left(A_{\mathrm{Co}} - A_{\mathrm{Gd}}\, e^{i\delta}\left(1 - e^{-\frac{t_{\mathrm{Gd}}}{\lambda_{\mathrm{mag}}}}\right)\right) e^{-\frac{t_{\mathrm{Gd}}}{\lambda_{\mathrm{diff}}}}, \qquad (1)$$

where A_{Co} and A_{Gd} are the dimensionless amplitudes of the precessions excited by the magnetic volume of Co and Gd, respectively. These then result in a combined precession with amplitude A_{FMR} and phase ϕ. Expressions for these two parameters can be derived, as is shown in Sec. III of Ref. [34]. Now $A_{\mathrm{Co}} = 1$ can be fixed by normalization, and $A_{\mathrm{Gd}} = 3.2$ and $\delta = -140^{\circ}$ are chosen to match the maximum of the amplitude and saturation of the phase, respectively. Within these constraints, valid values for the remaining parameters are found by manual adjustment, and are found to be $\lambda_{\mathrm{mag}} = 0.4 \pm 0.1$ nm and $\lambda_{\mathrm{diff}} = 2.0 \pm 0.2$ nm. The amplitude of the Gd-excited precession A_{Gd}, when corrected for the expected equivalent magnetic thickness of Gd (0.45 nm), gives a Gd contribution that is approximately 7 times larger per nm than that of Co. A complete understanding of this difference is outside of the scope of this work, but some factors of relevance are the differences in magnetization, the amount of magnetic moment lost during demagnetization, and the spin-wave excitation efficiency, which will be discussed later. The value for λ_{mag} closely matches the experimentally determined length scale for the loss of magnetization in Gd of ~0.45 nm [3]. We note that this length scale could also affect the rate of spin flip scattering, such that the parameter λ_{diff} might not provide a full description. Fitting the data for the FMR amplitude for thicknesses where Gd is expected to be paramagnetic (from 1.5 nm onwards) with an exponential function, indicated by the solid black line in Fig. 2(d) results in a $\lambda_{\mathrm{diff,Gd}}$ of 1.9 ± 0.2 nm, which has not been measured before to the best of our knowledge. The close agreement between the two descriptions indicates that the magnetic state is not very relevant for spin flip scattering in these weakly magnetic systems.

The reasonable agreement between experiments and calculations indicate that the most important elements of this complex system are captured by this simple model. However, the model can not capture the behavior we observe for a Co/Tb generation layer, as plotted in Figs. 2(c) and 2(e). Here we instead find only a rapid decrease of the amplitude with the addition of Tb. This could indicate a very short diffusion length λ_{diff} for Tb, which precludes any statements about the spin-current generation strength in Tb. We attribute this discrepancy to a larger degree of scattering of the mobile electrons in Tb due to the high SOC compared to Gd [36], leading to a loss of the spin information over shorter length scales.

B. THz mode

We measure the THz spin-waves as a function of RE thickness to investigate the spin-current generation on the ps timescale, and show a selection of the measurements for a Co/Gd injection layer in Fig. 3(a). Because THz mode excitation takes place on the same timescale as laser-induced demagnetization and spin-current generation, we disregard the first 2 ps of the data, in accordance with Ref. [27].

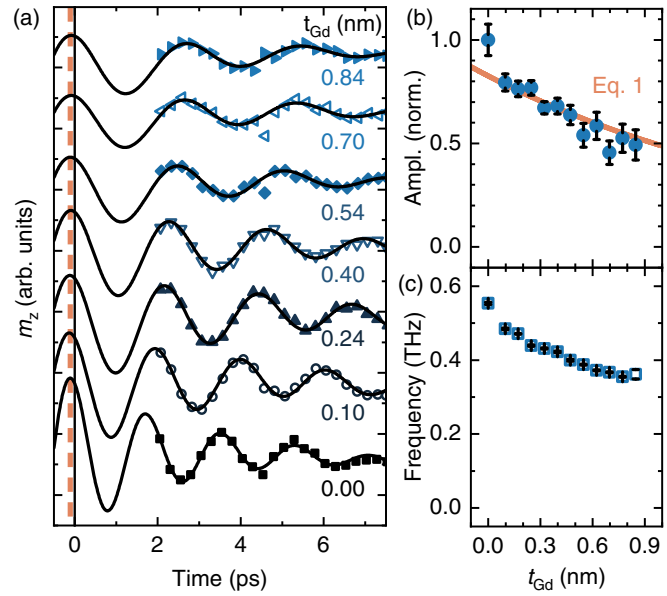

FIG. 3. (a) Measured THz mode for several Gd thicknesses, fitted with a damped cosine function. The orange dashed line indicates the spin-wave phase shift. (b) Spin-wave amplitude, orange line indicates a solution of Eq. 1 using $A_{\mathrm{Gd}} = 0$ and $\lambda_{\mathrm{diff,Gd}} = 1.9$ nm and (c) frequency as a function of Gd thickness.

We again used a damped cosine function to fit the data, indicated by the solid black lines, in order to extract the spin-wave amplitude, phase, and frequency. At around 1 nm, the signal-to-noise ratio is too low to extract spin-wave parameters reliably. The amplitude of the spin waves, which is plotted in Fig. 3(b), drops significantly with Gd thickness. Contrary to the behavior for the FMR mode, no initial rise of the amplitude due to a Gd contribution is observed. We therefore show the expression for the amplitude derived from Eq. (1) using $A_{\mathrm{Gd}} = 0$ and $\lambda_{\mathrm{diff,Gd}} = 1.9$ nm as the solid orange line in the figure, which is equivalent to an exponential decay describing only the spin diffusion due to Gd. The good agreement indicates that Gd is not actively contributing to the excitation of the THz mode, which shows that this mode is excited by the Co-dominated fast component of the generated spin current [38]. This is further confirmed by the observation that the spin-wave phase is independent of the Gd thickness, as indicated by the orange dashed line in Fig. 3(a). The same measurements are repeated for Tb and presented in Sec. IV of Ref. [34]. No significant difference between the THz spin-wave frequency and phase for the two materials is observed, again confirming the dominant role of Co in exciting these spin waves. However, a full analysis of the data is complicated by a more rapid decrease of the spin-wave amplitude with increasing Tb thickness, which could again be attributed to high spin-flip scattering due to SOC.

Contrary to our measurements of the FMR mode we observe a significant decrease of the THz spin-wave frequency for increasing Gd thickness, plotted in Fig. 3(c), which is not predicted by our simulations (see Sec. VI of Ref. [34]). In Sec. VII of Ref. [34], we discuss two mechanisms which we believe could cause a frequency shift of the THz mode. These consist of a growth related change of the exchange stiffness [26,39], and coupling between the THz mode in the

absorption layer and a ferrimagnetic exchange mode in the generation layer [40]. These mechanisms predict the same direction of the shift of the THz spin-wave frequency. In Sec. VII of Ref. [34], we also discuss a possible role of the so-called RKKY coupling between the layers. This coupling might be present with a Cu spacer layer [41], but is not found to significantly affect the behavior of the THz mode in our system. However, a full understanding of the origin of this frequency shift is beyond the scope of this work and requires further research.

IV. $s-d$ MODELLING

To better understand the mechanisms governing our observations, as well as the underlying physics in general, we modeled the generated spin current in the synthetic ferrimagnetic generation layer using an extension of the $s-d$ model [8,28–31,42,43]. This model describes the coupling of local spins, in this case the $3d$ and $4f$ electrons in the RE-TM ferrimagnet, to a system of itinerant spins (s electrons). The latter system includes diffusive spin transport, similar to Refs. [8,30,31]. Dissipation of the angular momentum carried by the itinerant electrons due to scattering events at interfaces or defects is taken into account with a phenomenological dissipation timescale. To model the experiments, we define a discretized material system consisting of a ferrimagnetic (Co/Gd) region and a nonmagnetic spacer layer (Cu). The Co/Gd bilayer is modeled in a layered manner, where the local Co and Gd concentration is sampled from a function that represents an intermixed transition from pure Co to Gd, similar to Ref. [44]. This process is discussed in Sec. V of Ref. [34]. Furthermore, the absorption layer is implemented as an ideal spin sink connected to the spacer layer, which is a valid assumption considering the experimental absorption layer thickness of 5 nm and the transverse spin diffusion length in Co of approximately 1 nm [26]. This allows us to calculate the absorbed spin current for varying composition of the Co/Gd layer. Using a linearized Landau-Lifshitz-Gilbert equation, including the antidamping spin-transfer torque exerted by the absorbed spin current, we calculate the absolute phase shift of the excited homogeneous precession. Although the used model includes multiple assumptions that disqualify any precise quantitative statements [34], it gives a complete description of the qualitative characteristics of the spin current and excited precession. Further details on the modeling, including all the used material parameters, are presented in Sec. V of Ref. [34].

In Fig. 4(a), we present traces of the modeled z component of the FMR mode excited by a Co(1) and a Co(1)/Gd(2) generation layer, in black and blue, respectively. Note that the amplitude of the FMR mode excited by pure Co has been multiplied by 10 for clarity, as it is significantly weaker than that excited by Co/Gd. This is likely a result of the assumptions made in the model, such as the simplistic description of optical absorption and the parameters chosen for Gd, as the exact shape of the spin current pulse strongly affects the excitation efficiency. Similar to the experimental results, our model shows a shift of the phase of the FMR mode when Gd is added to the generation layer. In Fig. 4(b), the absolute phase is plotted as a function of the effective Gd thickness $t_{\mathrm{eff,Gd}}$, which for our purposes is analogous to the Gd layer

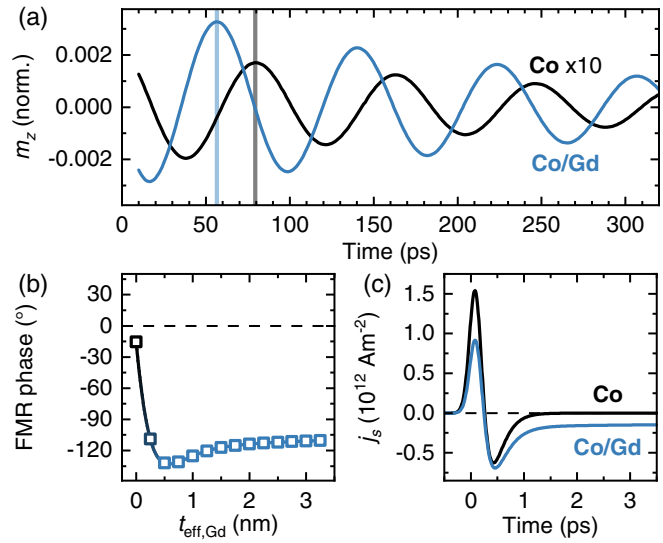

FIG. 4. (a) Calculated FMR mode excited by the spin current from a Co(1) (black) and Co(1)/Gd(2) (blue) generation layer. (b) Absolute phase of the excited FMR mode as a function of the effective thickness $t_{\mathrm{eff,Gd}}$ of the (generation) Gd layer. (c) Absorbed spin current as function of time generated by a Co (black) and a Co/Gd (blue) generation layers.

thickness, and is further described in Sec. V of Ref. [34]. The figure clearly shows a qualitative agreement with the experiments [Fig. 2(d)], with a shift of approximately 130° upon adding a few monolayers of Gd. The exact value of the phase shift can be explained by a combination of factors. Naively, one would expect a 180° phase shift if only the Gd spin-current would excite dynamics once it starts to dominate the total spin current. The actual shift however is lowered by the contribution of Co, as well as the relatively slow (type II [38]) magnetization dynamics of the Gd, as will be demonstrated in the following.

To clarify the origin of the observed phase shift, we plot the absorbed spin currents for a pure Co(1) injection layer and a Co(1)/Gd(2) bilayer calculated using the $s-d$ model in Fig. 4(c). The addition of Gd leads to changes in both the amplitude of the first, fast peak of the spin current, as well as a much longer negative tail. Both of these can be understood by the demagnetization behavior of Gd, as plotted in Fig. 1(b). The reduction of the amplitude of the first peak of the spin current is caused by the initial, relatively rapid demagnetization of Gd. At longer timescales, when the Co generated spin current is negligible, a long tail in the Co/Gd generated spin current is observed. This is in turn caused by the secondary, slower demagnetization of Gd, and results in a spin current that is mostly polarized in the opposite direction. This explains the abrupt phase jump in Figs. 2(d) and 4(b) for increasing Gd thickness. Moreover, the long duration of this component of the spin current gives rise to a deviation of the phase shift from 180°. This is to be expected, as the Gd demagnetization takes place over tens of ps, which is comparable to the precessional period (∼80 ps). The small increase of the phase from −130° to −110° that is observed in Fig. 4(b) for a further increase of the Gd thickness is attributed to an additional slowing down of the Gd magnetization dynamics.

More specifically, we find that transfer of angular momentum from the Co, which speeds up the Gd magnetization dynamics near the interface between Co and Gd, has a smaller total effect when the Gd thickness is increased.

In Sec. VI of Ref. [34], we show calculated traces of the THz mode for increasing Gd thickness. Our calculations indicate a phase shift of up to 10° when adding a 2-nm-thick Gd layer to a 1-nm-thick Co layer. Contrary to previous work [27], we were unable to resolve this potential phase shift, because the resolution is determined by the strength of the spin current and thus the total magnetic moment of the generation layer. In future research, Co/Gd multilayers could be used to study THz spin-wave generation in a rare-earth transition-metal ferrimagnetic system in more detail.

V. CONCLUSION

We have shown that examining the parameters of precessional modes excited by ultrafast optically generated spin currents can be a powerful tool to elucidate the behavior of these spin currents. Synthetic ferrimagnets offer a novel platform to systematically investigate these phenomena. The large discrepancy in spin current generation between Gd and Tb could shed new light on the relative difficulty of achieving AOS in systems containing only the latter as RE material. Using spin-wave modes with THz frequencies has additionally allowed us to probe the high-frequency component of the generated spin currents. Here we again find a link between the intrinsic speed of the magnetization dynamics and the behavior of the excited spin current. This gives additional weight to the notion that angular momentum which is lost during demagnetization can be transferred to mobile spins [8]. This notion also underlies the $s-d$ model, which we have successfully used to describe our experimental results. Our experiments give new insight in the magnetization dynamics of rare-earth materials, which could prove critical in future spintronic memory devices.

[1] C. D. Stanciu, F. Hansteen, A. V. Kimel, A. Kirilyuk, A. Tsukamoto, A. Itoh, and T. Rasing, All-Optical Magnetic Recording With Circularly Polarized Light, Phys. Rev. Lett. **99**, 047601 (2007).

[2] T. A. Ostler, J. Barker, R. F. L. Evans, R. W. Chantrell, U. Atxitia, O. Chubykalo-Fesenko, S. El Moussaoui, L. Le Guyader, E. Mengotti, L. J. Heyderman *et al.*, Ultrafast heating as a sufficient stimulus for magnetization reversal in a ferrimagnet, Nat. Commun. **3**, 666 (2012).

[3] M. L. M. Lalieu, M. J. G. Peeters, S. R. R. Haenen, R. Lavrijsen, and B. Koopmans, Deterministic all-optical switching of synthetic ferrimagnets using single femtosecond laser pulses, Phys. Rev. B **96**, 220411(R) (2017).

[4] L. Avilés-Félix, L. Álvaro-Gómez, G. Li, C. Davies, A. Olivier, M. Rubio-Roy, S. Auffret, A. Kirilyuk, A. Kimel, T. Rasing *et al.*, Integration of Tb/Co multilayers within optically switchable perpendicular magnetic tunnel junctions, AIP Adv. **9**, 125328 (2019).

[5] A. V. Kimel and M. Li, Writing magnetic memory with ultrashort light pulses, Nat. Rev. Mater. **4**, 189 (2019).

[6] I. Radu, K. Vahaplar, C. Stamm, T. Kachel, N. Pontius, H. Dürr, T. Ostler, J. Barker, R. Evans, R. Chantrell *et al.*, Transient ferromagnetic-like state mediating ultrafast reversal of antiferromagnetically coupled spins, Nature (London) **472**, 205 (2011).

[7] M. Battiato, K. Carva, and P. M. Oppeneer, Superdiffusive Spin Transport as a Mechanism of Ultrafast Demagnetization, Phys. Rev. Lett. **105**, 027203 (2010).

[8] G.-M. Choi, B.-C. Min, K.-J. Lee, and D. G. Cahill, Spin current generated by thermally driven ultrafast demagnetization, Nat. Commun. **5**, 4334 (2014).

[9] G. Malinowski, F. Dalla Longa, J. Rietjens, P. Paluskar, R. Huijink, H. Swagten, and B. Koopmans, Control of speed and efficiency of ultrafast demagnetization by direct transfer of spin angular momentum, Nat. Phys. **4**, 855 (2008).

[10] A. Melnikov, I. Razdolski, T. O. Wehling, E. T. Papaioannou, V. Roddatis, P. Fumagalli, O. Aktsipetrov, A. I. Lichtenstein, and U. Bovensiepen, Ultrafast Transport of Laser-Excited Spin-Polarized Carriers in Au/Fe/Mgo (001), Phys. Rev. Lett. **107**, 076601 (2011).

[11] D. Rudolf, M. Battiato, R. Adam, J. M. Shaw, E. Turgut, P. Maldonado, S. Mathias, P. Grychtol, H. T. Nembach, T. J. Silva *et al.*, Ultrafast magnetization enhancement in metallic multilayers driven by superdiffusive spin current, Nat. Commun. **3**, 1037 (2012).

[12] J. Hurst, P.-A. Hervieux, and G. Manfredi, Spin current generation by ultrafast laser pulses in ferromagnetic nickel films, Phys. Rev. B **97**, 014424 (2018).

[13] J. K. Dewhurst, P. Elliott, S. Shallcross, E. K. Gross, and S. Sharma, Laser-induced intersite spin transfer, Nano Lett. **18**, 1842 (2018).

[14] R. Rouzegar, L. Brandt, L. Nadvornik, D. Reiss, A. Chekhov, O. Gueckstock, C. In, M. Wolf, T. Seifert, P. Brouwer *et al.*, Laser-induced terahertz spin transport in magnetic nanostructures arises from the same force as ultrafast demagnetization, arXiv:2103.11710.

[15] P. Jiménez-Cavero, O. Gueckstock, L. Nádvorník, I. Lucas, T. S. Seifert, M. Wolf, R. Rouzegar, P. W. Brouwer, S. Becker, G. Jakob *et al.*, Transition of laser-induced terahertz spin currents from torque-to conduction-electron-mediated transport, Phys. Rev. B **105**, 184408 (2022).

[16] Y. L. W. van Hees, P. van de Meugheuvel, B. Koopmans, and R. Lavrijsen, Deterministic all-optical magnetization writing facilitated by non-local transfer of spin angular momentum, Nat. Commun. **11**, 3835 (2020).

[17] S. Iihama, Y. Xu, M. Deb, G. Malinowski, M. Hehn, J. Gorchon, E. E. Fullerton, and S. Mangin, Single-shot multi-level all-optical magnetization switching mediated by spin transport, Adv. Mater. **30**, 1804004 (2018).

[18] J. Igarashi, Q. Remy, S. Iihama, G. Malinowski, M. Hehn, J. Gorchon, J. Hohlfeld, S. Fukami, H. Ohno, and S. Mangin, Engineering single-shot all-optical switching of ferromagnetic materials, Nano Lett. **20**, 8654 (2020).

[19] Q. Remy, J. Igarashi, S. Iihama, G. Malinowski, M. Hehn, J. Gorchon, J. Hohlfeld, S. Fukami, H. Ohno, and S. Mangin, Energy efficient control of ultrafast spin current to induce single

femtosecond pulse switching of a ferromagnet, Adv. Sci. **7**, 2001996 (2020).

[20] L. Avilés-Félix, A. Olivier, G. Li, C. S. Davies, L. Álvaro-Gómez, M. Rubio-Roy, S. Auffret, A. Kirilyuk, A. Kimel, T. Rasing *et al.*, Single-shot all-optical switching of magnetization in Tb/Co multilayer-based electrodes, Sci. Rep. **10**, 5211 (2020).

[21] M. Beens, M. L. M. Lalieu, A. J. M. Deenen, R. A. Duine, and B. Koopmans, Comparing all-optical switching in synthetic-ferrimagnetic multilayers and alloys, Phys. Rev. B **100**, 220409(R) (2019).

[22] G.-M. Choi and B.-C. Min, Laser-driven spin generation in the conduction bands of ferrimagnetic metals, Phys. Rev. B **97**, 014410 (2018).

[23] D. Haskel, G. Srajer, J. C. Lang, J. Pollmann, C. S. Nelson, J. S. Jiang, and S. D. Bader, Enhanced Interfacial Magnetic Coupling of Gd/Fe Multilayers, Phys. Rev. Lett. **87**, 207201 (2001).

[24] A. J. Schellekens, K. C. Kuiper, R. R. J. C. De Wit, and B. Koopmans, Ultrafast spin-transfer torque driven by femtosecond pulsed-laser excitation, Nat. Commun. **5**, 4333 (2014).

[25] I. Razdolski, A. Alekhin, N. Ilin, J. P. Meyburg, V. Roddatis, D. DIesing, U. Bovensiepen, and A. Melnikov, Nanoscale interface confinement of ultrafast spin transfer torque driving non-uniform spin dynamics, Nat. Commun. **8**, 15007 (2017).

[26] M. L. M. Lalieu, P. L. J. Helgers, and B. Koopmans, Absorption and generation of femtosecond laser-pulse excited spin currents in noncollinear magnetic bilayers, Phys. Rev. B **96**, 014417 (2017).

[27] T. Lichtenberg, M. Beens, M. H. Jansen, B. Koopmans, and R. A. Duine, Probing optically induced spin currents using terahertz spin waves in noncollinear magnetic bilayers, Phys. Rev. B **105**, 144416 (2022).

[28] V. N. Gridnev, Ultrafast heating-induced magnetization switching in ferrimagnets, J. Phys.: Condens. Matter **28**, 476007 (2016).

[29] E. G. Tveten, A. Brataas, and Y. Tserkovnyak, Electron-magnon scattering in magnetic heterostructures far out of equilibrium, Phys. Rev. B **92**, 180412(R) (2015).

[30] I.-H. Shin, B.-C. Min, B.-K. Ju, and G.-M. Choi, Ultrafast spin current generated by electron–magnon scattering in bulk of ferromagnets, Jpn. J. Appl. Phys. **57**, 090307 (2018).

[31] M. Beens, R. A. Duine, and B. Koopmans, S- D model for local and nonlocal spin dynamics in laser-excited magnetic heterostructures, Phys. Rev. B **102**, 054442 (2020).

[32] A. J. Schellekens, N. De Vries, J. Lucassen, and B. Koopmans, Exploring laser-induced interlayer spin transfer by an all-optical method, Phys. Rev. B **90**, 104429 (2014).

[33] H. Eichler, D. Langhans, and F. Massmann, Coherence peaks in picosecond sampling experiments, Opt. Commun. **50**, 117 (1984).

[34] See Supplemental Material at http://link.aps.org/supplemental/10.1103/PhysRevB.106.094436 for (i) additional experimental details [45], (ii) details on the transfer matrix calculations [46–48], (iii) a derivation of the amplitude and phase of $\tilde{A}_{\mathrm{FMR}}$, (iv) THz spin waves excited by Co/Tb, (v) a detailed discussion of the $s-d$ modeling, (vi) THz spin waves calculated using the $s-d$ model, (vii) further details on the THz spin-wave frequency shift [39–41,49–51].

[35] M. Wietstruk, A. Melnikov, C. Stamm, T. Kachel, N. Pontius, M. Sultan, C. Gahl, M. Weinelt, H. A. Dürr, and U. Bovensiepen, Hot-Electron-Driven Enhancement of Spin-Lattice Coupling in Gd and Tb 4*f* Ferromagnets Observed by Femtosecond X-Ray Magnetic Circular Dichroism, Phys. Rev. Lett. **106**, 127401 (2011).

[36] B. Frietsch, A. Donges, R. Carley, M. Teichmann, J. Bowlan, K. Döbrich, K. Carva, D. Legut, P. M. Oppeneer, U. Nowak *et al.*, The role of ultrafast magnon generation in the magnetization dynamics of rare-earth metals, Sci. Adv. **6**, eabb1601 (2020).

[37] C. C. Katsidis and D. I. Siapkas, General transfer-matrix method for optical multilayer systems with coherent, partially coherent, and incoherent interference, Appl. Opt. **41**, 3978 (2002).

[38] B. Koopmans, G. Malinowski, F. Dalla Longa, D. Steiauf, M. Fähnle, T. Roth, M. Cinchetti, and M. Aeschlimann, Explaining the paradoxical diversity of ultrafast laser-induced demagnetization, Nat. Mater. **9**, 259 (2010).

[39] C. Eyrich, A. Zamani, W. Huttema, M. Arora, D. Harrison, F. Rashidi, D. Broun, B. Heinrich, O. Mryasov, M. Ahlberg *et al.*, Effects of substitution on the exchange stiffness and magnetization of Co films, Phys. Rev. B **90**, 235408 (2014).

[40] B. Divinskiy, G. Chen, S. Urazhdin, S. O. Demokritov, and V. E. Demidov, Effects of Spin-Orbit Torque On the Ferromagnetic and Exchange Spin-Wave Modes in Ferrimagnetic Co-Gd Alloy, Phys. Rev. Appl. **14**, 044016 (2020).

[41] P. Bruno and C. Chappert, Oscillatory Coupling Between Ferromagnetic Layers Separated By a Nonmagnetic Metal Spacer, Phys. Rev. Lett. **67**, 1602 (1991).

[42] Ł. Cywiński and L. J. Sham, Ultrafast demagnetization in the $sp-d$ model: A theoretical study, Phys. Rev. B **76**, 045205 (2007).

[43] A. Manchon, Q. Li, L. Xu, and S. Zhang, Theory of laser-induced demagnetization at high temperatures, Phys. Rev. B **85**, 064408 (2012).

[44] M. Beens, M. L. M. Lalieu, R. A. Duine, and B. Koopmans, The role of intermixing in all-optical switching of synthetic-ferrimagnetic multilayers, AIP Adv. **9**, 125133 (2019).

[45] B. Koopmans, M. Van Kampen, J. Kohlhepp, and W. De Jonge, Femtosecond spin dynamics of epitaxial Cu(111)/Ni/Cu wedges, J. Appl. Phys. **87**, 5070 (2000).

[46] S. J. Byrnes, Multilayer optical calculations, arXiv:1603.02720.

[47] L. A. Akashev, N. A. Popov, and V. G. Shevchenko, Optical properties of gadolinium in the condensed state, High Temp. **57**, 49 (2019).

[48] Y. Xu, M. Hehn, W. Zhao, X. Lin, G. Malinowski, and S. Mangin, From single to multiple pulse all-optical switching in gdfeco thin films, Phys. Rev. B **100**, 064424 (2019).

[49] S. P. Vernon, S. M. Lindsay, and M. B. Stearns, Brillouin scattering from thermal magnons in a thin Co film, Phys. Rev. B **29**, 4439 (1984).

[50] N. Thiyagarajah, S. Bae, H. W. Joo, Y. C. Han, and J. Kim, Effects of perpendicular anisotropy on the interlayer coupling in perpendicularly magnetized [Pd/Co]/Cu/[Co/Pd] spin valves, Appl. Phys. Lett. **92**, 062504 (2008).

[51] Y. Tserkovnyak, A. Brataas, G. E. Bauer, and B. I. Halperin, Nonlocal magnetization dynamics in ferromagnetic heterostructures, Rev. Mod. Phys. **77**, 1375 (2005).